Supplementary Information Inventory:

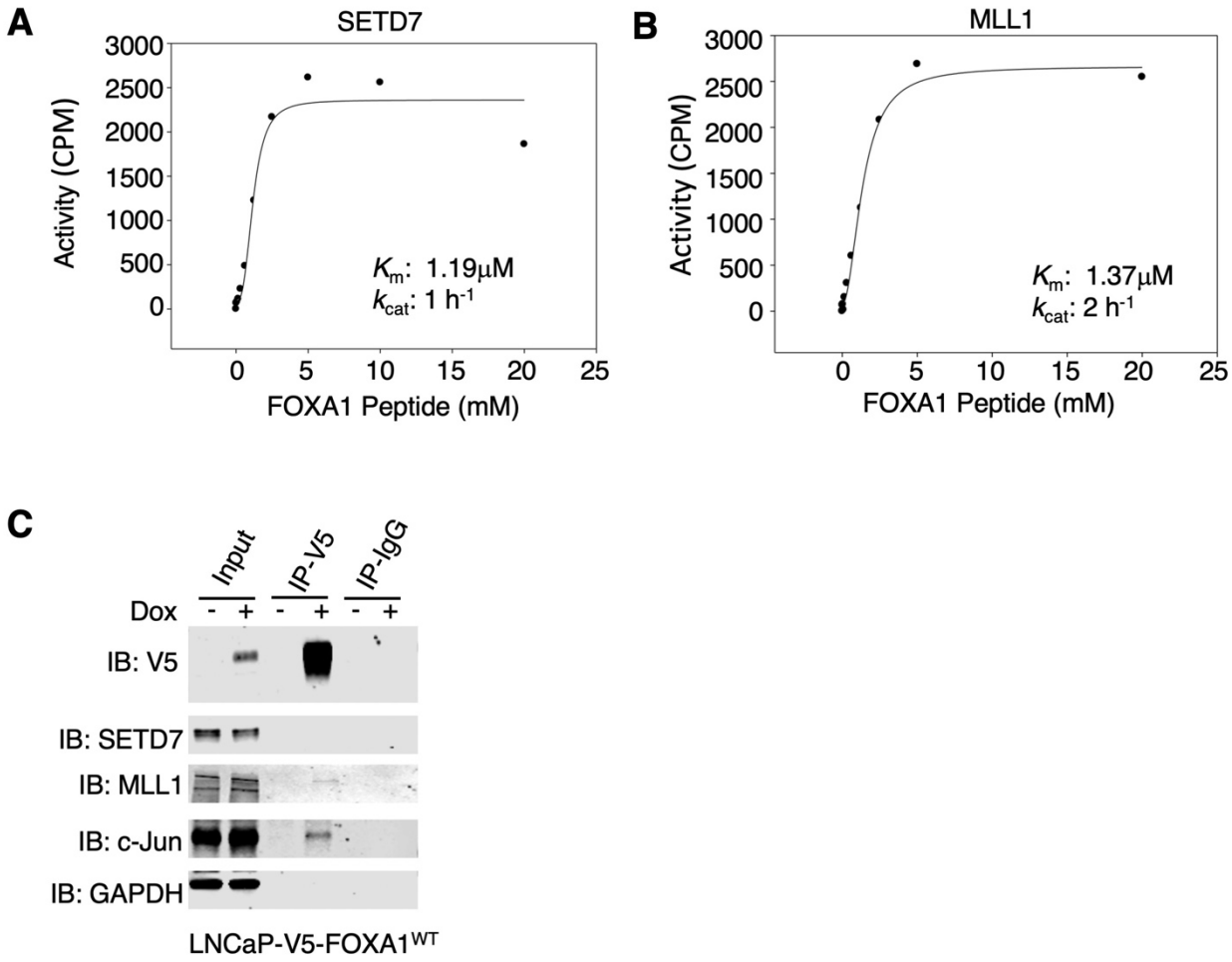

Figure S1. Validation of SETD7 and MLL1 activity

(**A, B**) Validation of SETD7 (A) and MLL1 (B) activity using 1μM methyltransferase proteins titrated at a series of FOXA1 peptide concentrations. (**C**) Immunoblotting for SETD7 and MLL1 in V5-FOXA1-overexpressing LNCaP cells immunoprecipitated with V5 and treated with or without doxycycline (0.5μg/ml).

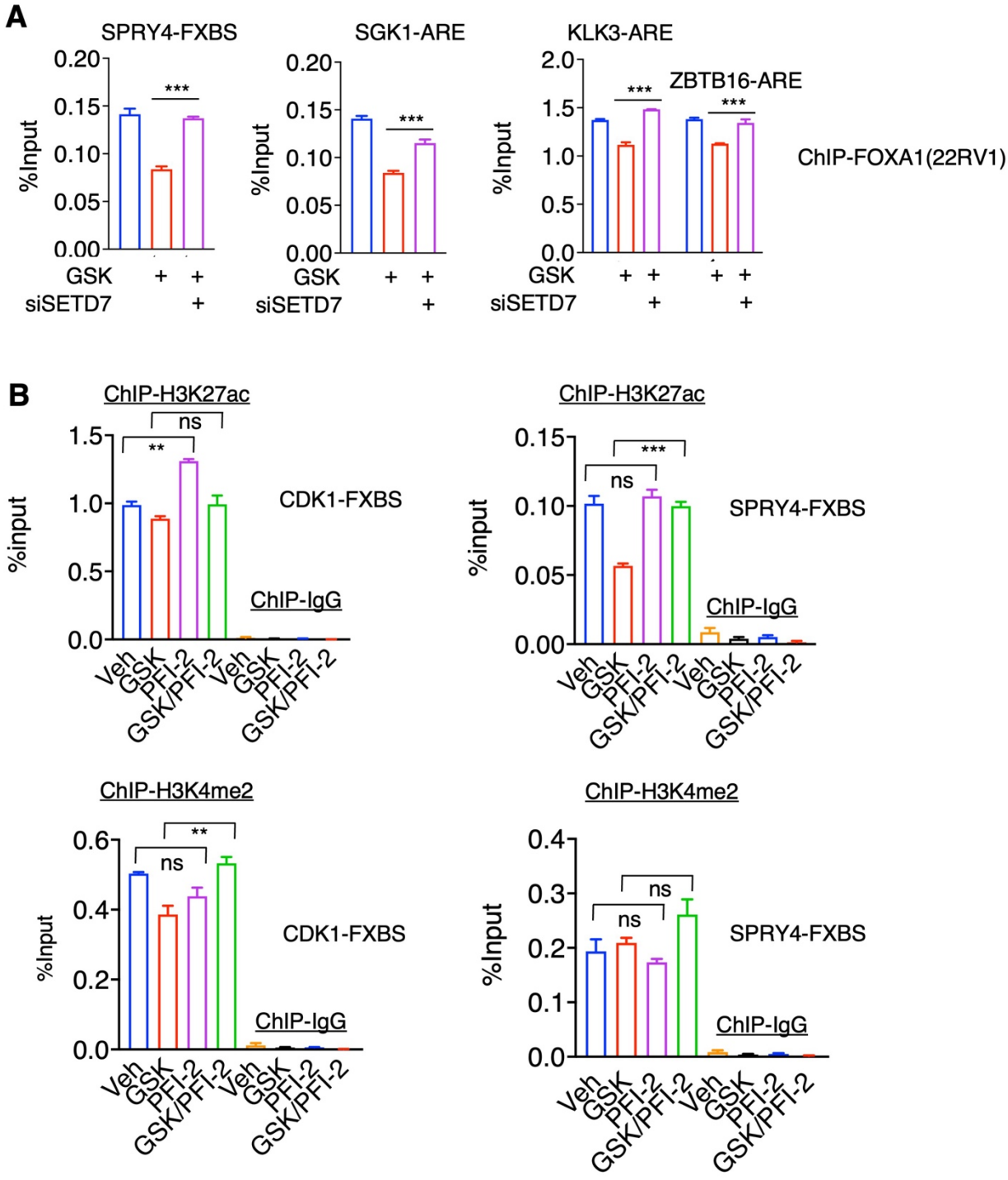
A
SPRY4-FXBS
SGK1-ARE
KLK3-ARE
ZBTB16-ARE
%Input
0.20
0.15
0.10
0.05
0.00
2.0
1.5
1.0
0.5
0.0
***
GSK
siSETD7
+
ChIP-FOXA1(22RV1)
B
ChIP-H3K27ac
ChIP-H3K4me2
CDK1-FXBS
SPRY4-FXBS
ChIP-IgG
%input
%Input
ns
**
0.6
0.4
0.3
Veh
GSK
PFI-2
GSK/PFI-2

Figure S2. Change of histone markers at FOXA1 binding sites in response to LSD1 and SETD7 inhibition (**A**) ChIP–qPCR for FOXA1 at indicated FOXA1 binding sites (FXBSs) in 22Rv1cells transfected with or without siSETD7 and with or without LSD1 inhibitor (GSK2879552, 100μM). (**B**) ChIP–qPCR for H3K27ac and H3K4me2 at Indicated FOXA1 binding sites in LNCaP treated with GSK2879552 (100μM) or PFI-2 (1μM) alone or the combination for 4h.

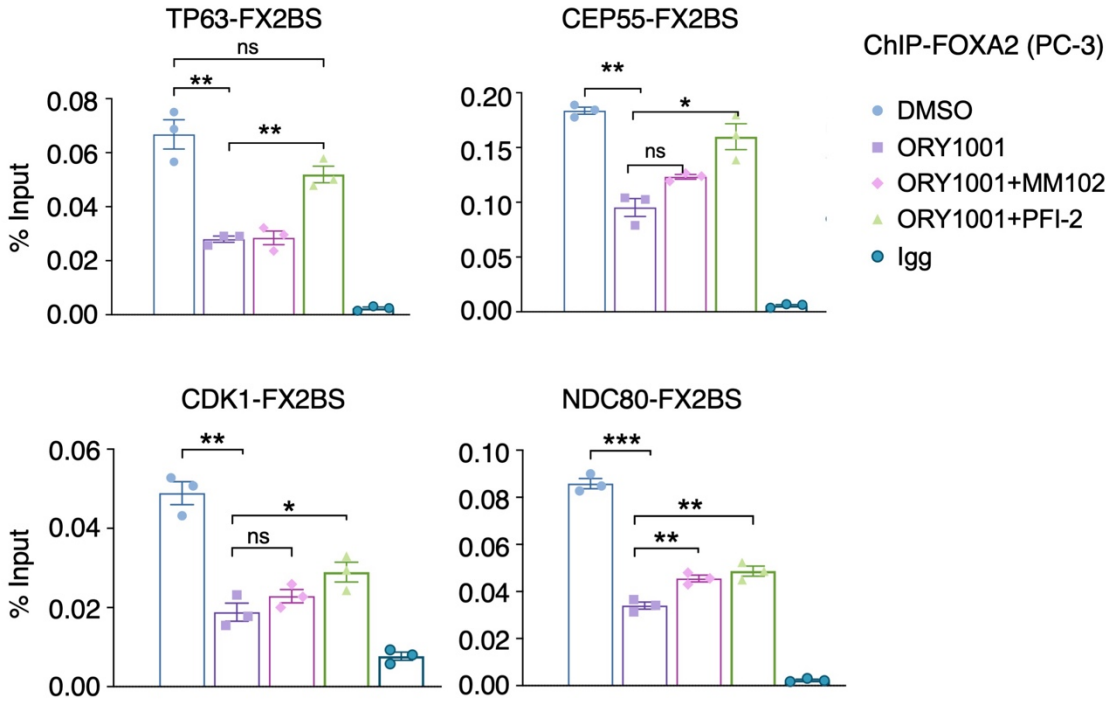

Figure S3. SETD7 inhibition partially rescues LSD1-i-disrupted chromatin binding of FOXA2

ChIP–qPCR for FOXA2 (antibody purchased from Millipore, 17-10258) at indicated FOXA2 binding sites (FX2BSs) in PC-3 cells treated with ORY1001 or its combination with MM102 (50μM) or PFI-2 (1μM) for 4h.

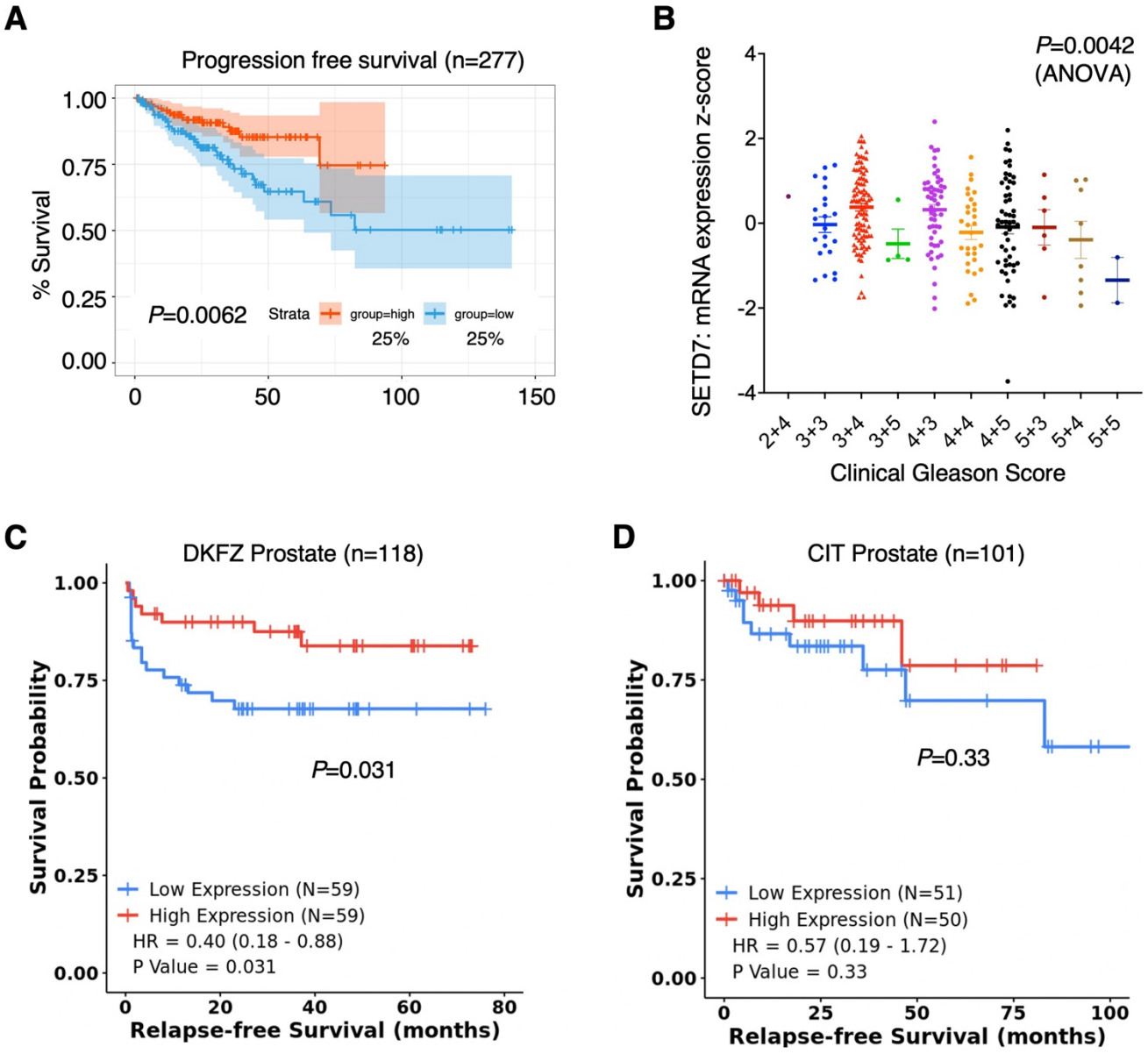

Figure S4. Decreased SETD7 expression is associated with more aggressive PCa

(**A**) Kaplan–Meier curve for the progression-free survival in the tumors with higher *SETD7* expression (red, the top 25%) versus with lower expression (blue, the bottom 25%) (TCGA dataset). (**B**) *SETD7* expression in PCa with different Gleason scores (TCGA). (**C**, **D**) Kaplan–Meier curve for the relapse-free survival in PCa tumors with higher *SETD7* expression (red, the top 50%) versus with lower expression (blue, the bottom 50%) in DKFZ (1) and CIT (2) datasets.

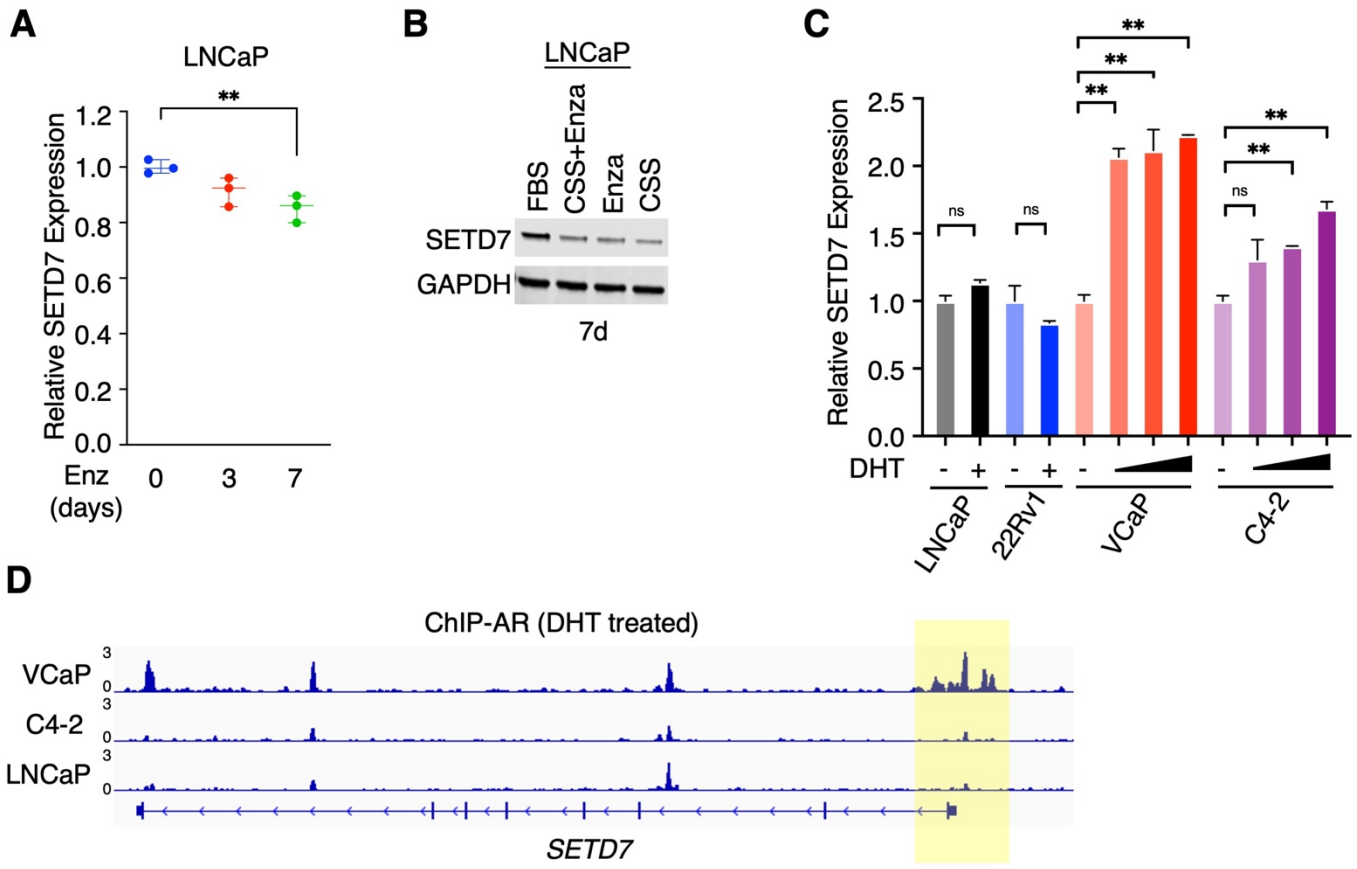

Figure S5. SETD7 expression is decreased by androgen deprivation treatments

(**A**) qRT-PCR for *SETD7* expression in LNCaP cells treated with enzalutamide (10μM) for 0, 3, or 7 days. (**B**) Immunoblotting for SETD7 in LNCaP cells treated with enzalutamide, hormone-depletion (CSS), or enzalutamide plus hormone-depletion. (**C**) qRT-PCR for *SETD7* expression in PCa cell lines treated with vehicle or DHT (10nM for LNCaP and 22Rv1; 0.1, 1, or 10nM for VCaP and C4-2). (D) Genome view of AR binding (ChIP-seq) in VCaP, C4-2, and LNCaP cells treated with 10nM DHT (3-5).

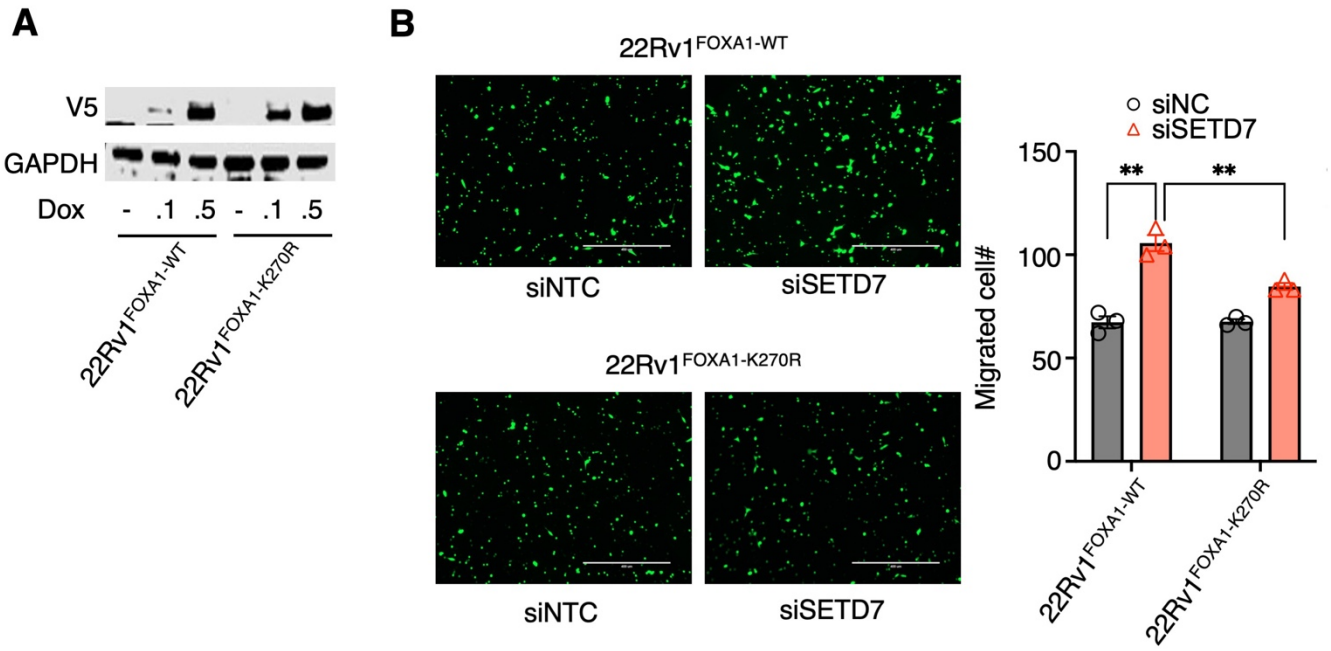

Figure S6. SETD7 silencing induced cell migration is dependent on K270 methylation of FOXA1

(**A**) Immunoblotting for V5 in V5-FOXA1^{WT} or V5-FOXA1^{K270R}-overexpressing (doxycycline-regulated) 22Rv1 cells treated with 0, 01, or 0.5μg/ml doxycycline. (**B**) Migration assay in these stable cells (induced with 0.5μg/ml doxycycline) transfected with siNTC or siSETD7.

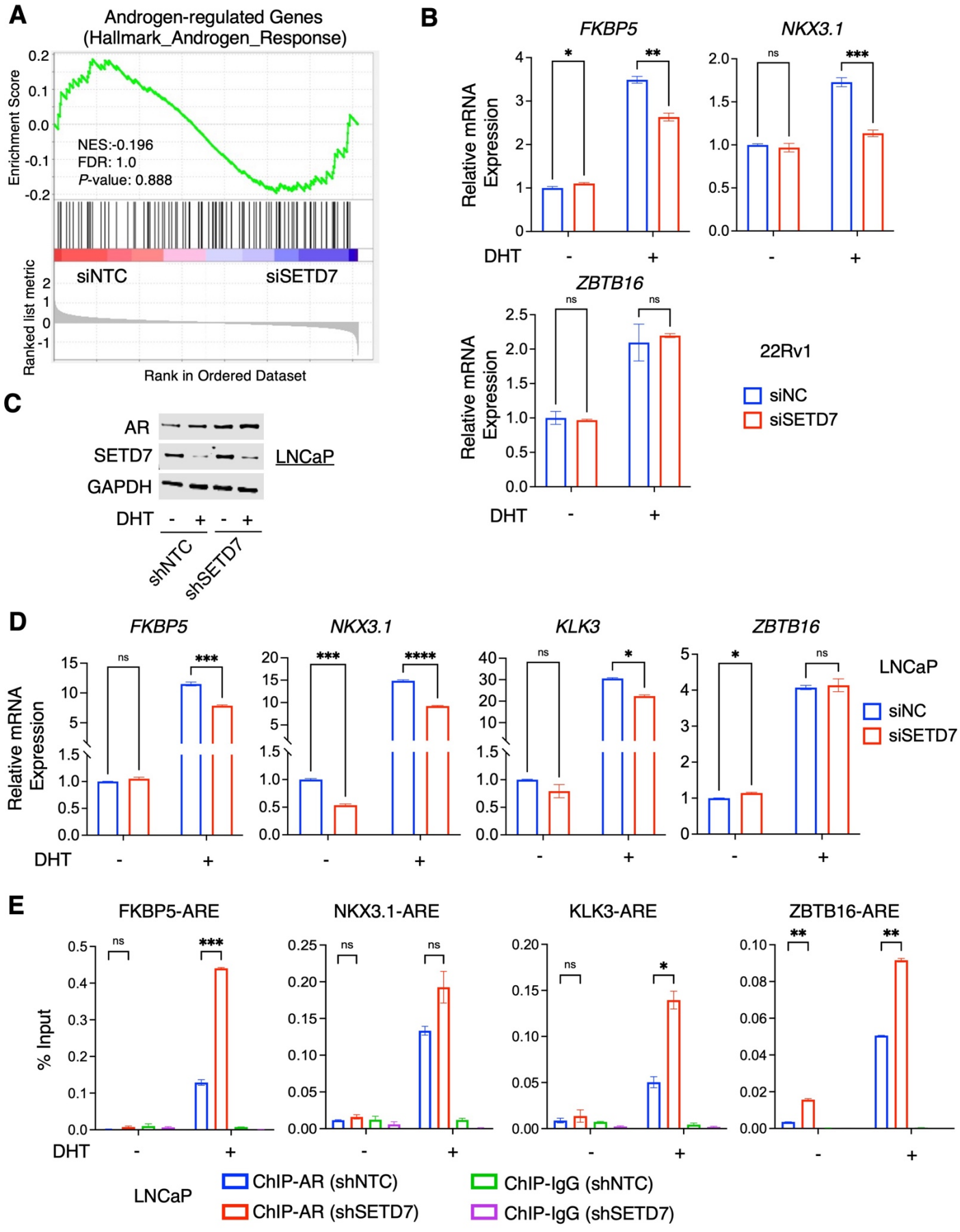
A
Androgen-regulated Genes
(Hallmark_Androgen_Response)
Enrichment Score
NES:-0.196
FDR: 1.0
P-value: 0.888
siNTC
siSETD7
Ranked list metric
Rank in Ordered Dataset
B
FKBP5
NKX3.1
ZBTB16
Relative mRNA Expression
DHT
22Rv1
siNC
siSETD7
C
AR
SETD7
GAPDH
LNCaP
DHT
shNTC
shSETD7
D
FKBP5
NKX3.1
KLK3
ZBTB16
Relative mRNA Expression
LNCaP
siNC
siSETD7
DHT
E
FKBP5-ARE
NKX3.1-ARE
KLK3-ARE
ZBTB16-ARE
% Input
DHT
LNCaP
ChIP-AR (shNTC)
ChIP-AR (shSETD7)
ChIP-IgG (shNTC)
ChIP-IgG (shSETD7)

Figure S7. SETD7 silencing enhances AR chromatin binding but not its transcriptional activity

(**A**) GSEA of hallmark_androgen_response genes for SETD7-activated and repressed genes. (**B**, **D**) qRT-PCR for AR-regulated genes in 22Rv1 cells (B) or LNCaP cells (D) treated with/out DHT and transfected with siNTC or siSETD7. (**C**) Immunoblotting for AR and SETD7 in LNCaP cells stably infected with shNTC or shSETD7. (**E**) ChIP-qPCR of AR at indicated AR binding sites in LNCaP cells treated with/out DHT and stably infected with lentiviral shNTC or shSETD7.

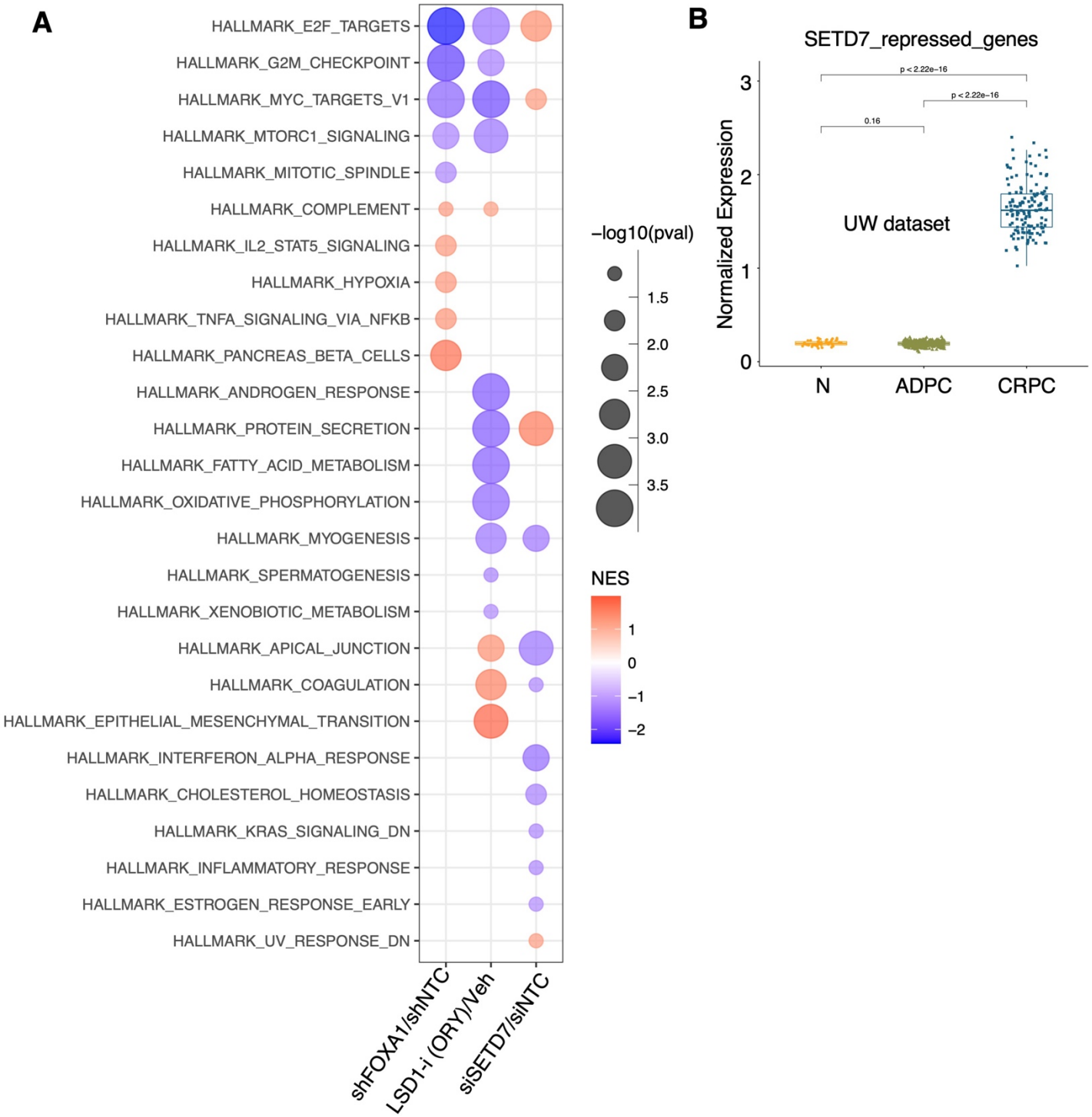
A
HALLMARK_E2F_TARGETS
HALLMARK_G2M_CHECKPOINT
HALLMARK_MYC_TARGETS_V1
HALLMARK_MTORC1_SIGNALING
HALLMARK_MITOTIC_SPINDLE
HALLMARK_COMPLEMENT
HALLMARK_IL2_STAT5_SIGNALING
HALLMARK_HYPOXIA
HALLMARK_TNFA_SIGNALING_VIA_NFKB
HALLMARK_PANCREAS_BETA_CELLS
HALLMARK_ANDROGEN_RESPONSE
HALLMARK_PROTEIN_SECRETION
HALLMARK_FATTY_ACID_METABOLISM
HALLMARK_OXIDATIVE_PHOSPHORYLATION
HALLMARK_MYOGENESIS
HALLMARK_SPERMATOGENESIS
HALLMARK_XENOBIOTIC_METABOLISM
HALLMARK_APICAL_JUNCTION
HALLMARK_COAGULATION
HALLMARK_EPITHELIAL_MESENCHYMAL_TRANSITION
HALLMARK_INTERFERON_ALPHA_RESPONSE
HALLMARK_CHOLESTEROL_HOMEOSTASIS
HALLMARK_KRAS_SIGNALING_DN
HALLMARK_INFLAMMATORY_RESPONSE
HALLMARK_ESTROGEN_RESPONSE_EARLY
HALLMARK_UV_RESPONSE_DN
shFOXA1/shNTC
LSD1-i (ORY)/Veh
siSETD7/siNTC
−log10(pval)
1.5
2.0
2.5
3.0
3.5
NES
1
0
−1
−2
B
SETD7_repressed_genes
Normalized Expression
p < 2.22e−16
p < 2.22e−16
0.16
UW dataset
N
ADPC
CRPC

Figure S8. SETD7 function is opposite to LSD1 and FOXA1

(**A**) GSEA dot plot for shFOXA1 versus shNTC (GSE37314), LSD1 inhibitor (ORY-1001) vs vehicle-treated (GSE209889), and siSETD7 versus siNTC in 22Rv1 cells using hallmark gene sets. (**B**) SETD7-repressed genes in UW mCRPC dataset (6).

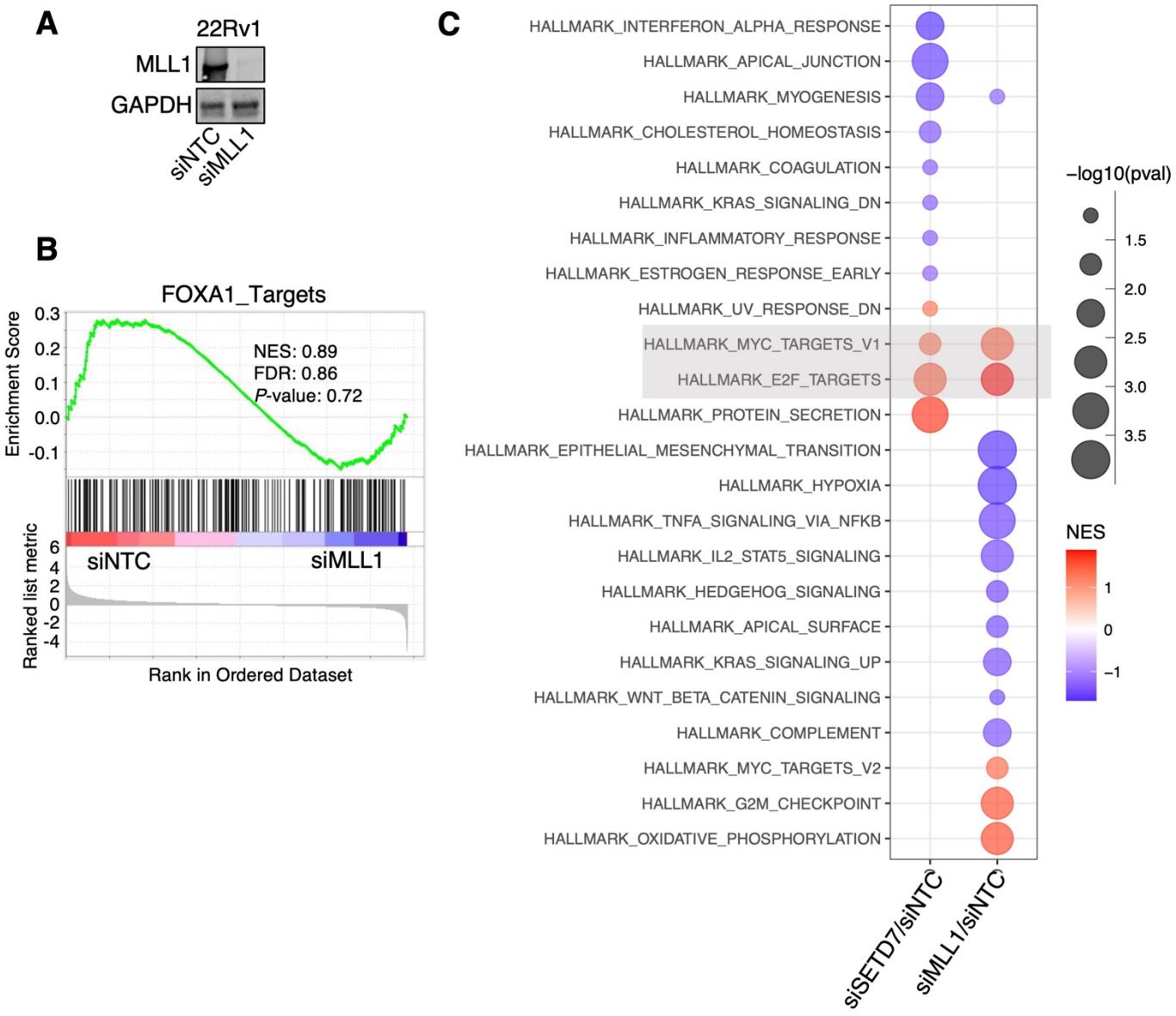

Figure S9. MLL1-regulated genes are not enriched for FOXA1 targets.

(**A**) Immunoblotting for MLL1 in 22RV1 cells transfected with siMLL1 or siNTC. (**B**) GSEA plot for the association of FOXA1 targets with siMLL-regulated genes. (**C**) GSEA dot plot for functional enrichment of differentially regulated genes in 22Rv1 cells transfected with siSETD7 versus siNTC or siMLL1 versus siNTC using hallmark gene sets.

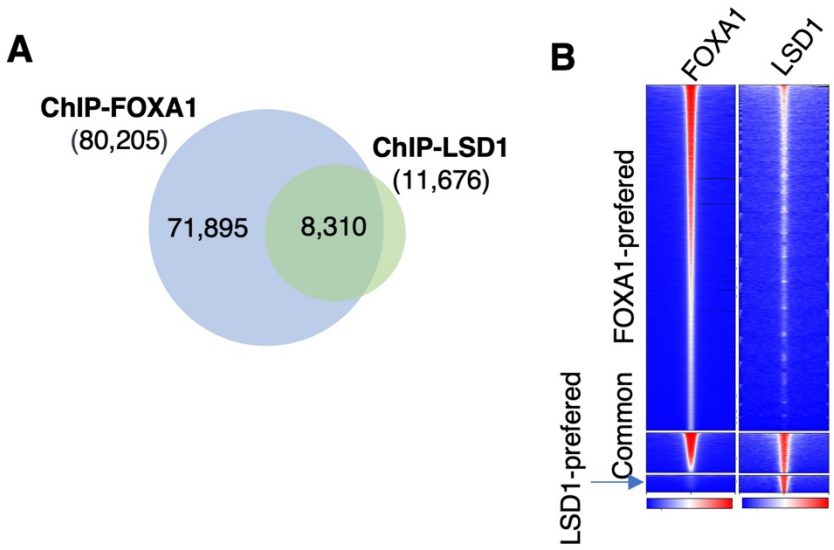

Figure S10. FOXA1 and LSD1 chromatin bindings sites are overwhelmingly overlapped

(A) Venn diagram for previously published ChIP-LSD1 peaks and ChIP-FOXA1 peaks in LNCaP cells. (**B**) Heatmap view for LSD1 binding and FOXA1 binding.

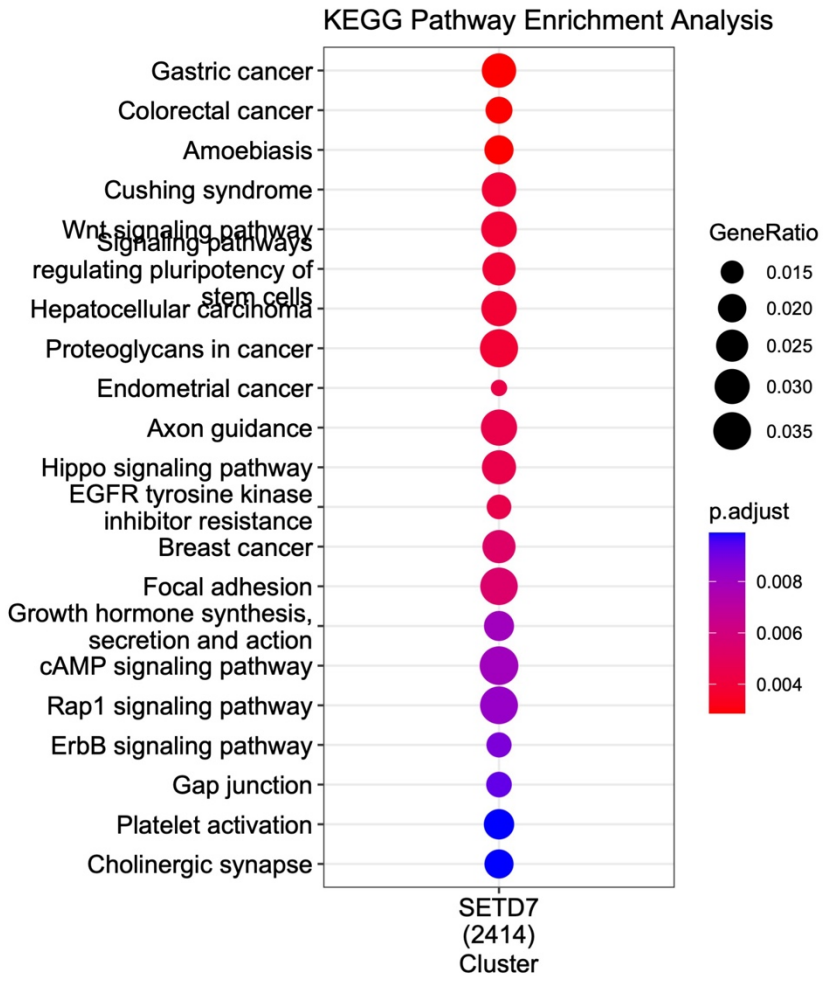

Figure S11. SETD7 binding peaks are enriched for genes promoting cancer development

KEGG pathway analysis for genes containing nearby SETD7 binding peaks.

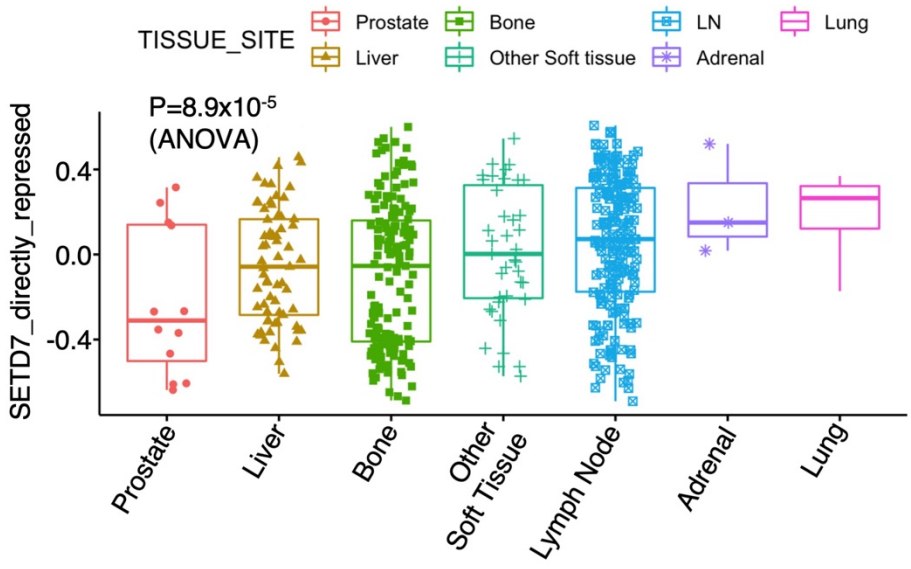

Figure S12. SETD7-directly-repressed genes are highly expressed in metastasis sites

Box plot for the average expression of identified SETD7-directly-repressed genes in metastasis sites of CRPC using SU2C dataset.

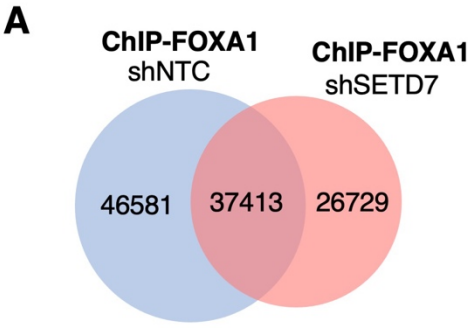

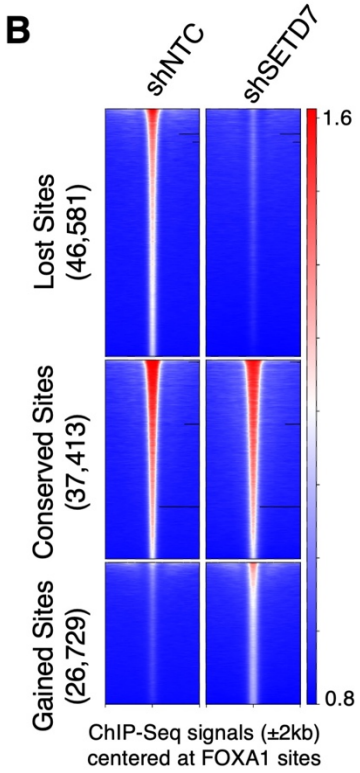

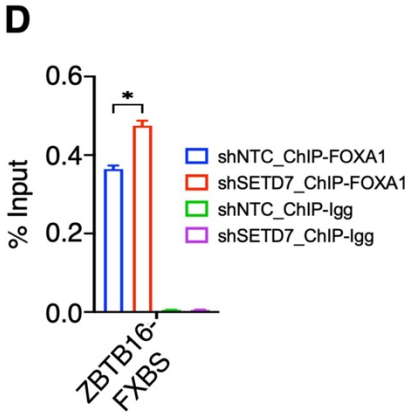

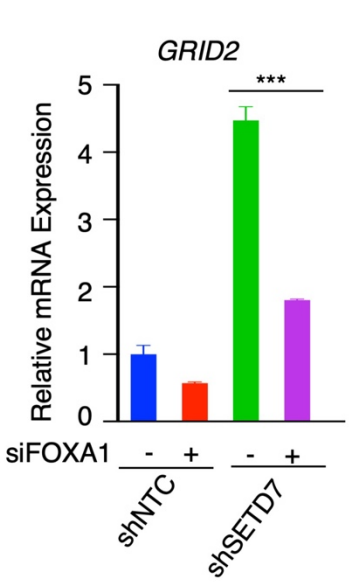

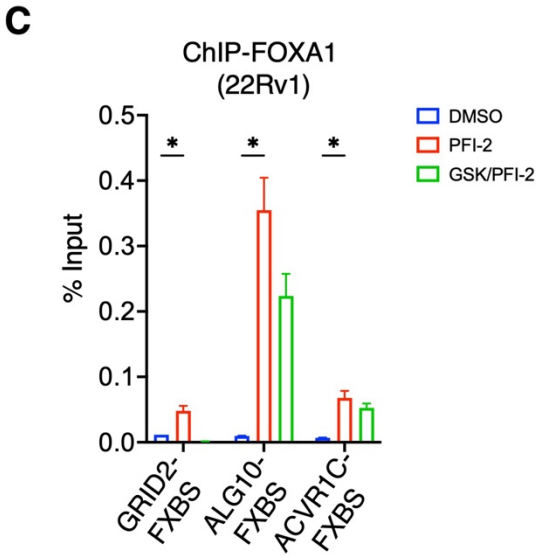

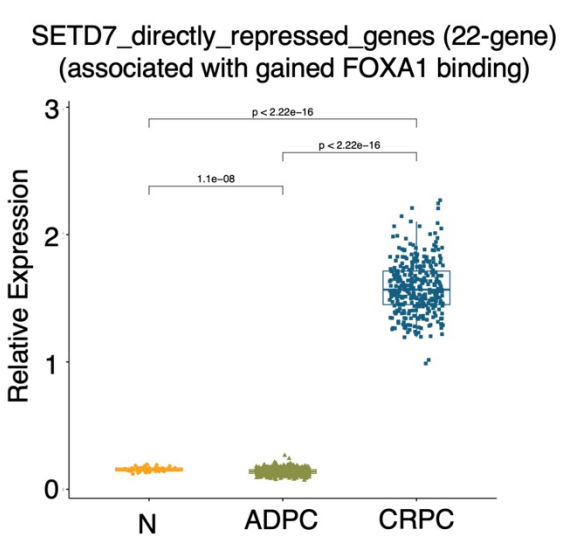

E

Gene Name			
GRID2	LINC01192	ZPLD1	A2M
ERC2	MTMR7	PTPRR	COMMD10
PEX5L	STEAP1B	ESRRG	GUCY1A2
ALG10	SNX16	SLC16A7	PTGS2
ZBBX	LRR1Q1	MICU3	
PRDM5	ZBTB41	LNC01205	

Figure S13. FOXA1 is reprogrammed in PCa cells with loss of SETD7 expression

(A) Venn diagram for FOXA1 binding sites (FOXA1 ChIP-seq) in 22Rv1 cells stably expressing shNTC or shSETD7. (**B**) Heatmap view for FOXA1 binding intensity at lost, reserved, and gained FOXA1 binding sites. (**C**) ChIP-qPCR of FOXA1 at gained sites in 22Rv1 cells treated with PFI-2 (1μM) or PFI-2 plus GSK2879552 (100μM). (**D**) ChIP-qPCR of FOXA1 at ZBTB16 enhancer (containing AR and FOXA1 binding motifs). (**E**) List of 22 SETD7-directly-repressed genes associated with gained FOXA1 binding. (**F**) qRT-PCR for *GRID2* expression in 22Rv1 stable cells with SETD7 silencing transfected with siNTC or siFOXA1. (**G**) Box plots for SETD7-directly-repressed genes in normal and primary PCa samples (TCGA) and mCRPC samples (SU2C).

SETD7_Repressed (2-fold)		SETD7-Activated (2-fold)	SETD7_Directly_Repressed (BETA)							
EIF1AXP1	YWHAZP10	MMP23B	GUCY1A2	SNX10	CAPZA2	CAAP1	EDEM3	ZBTB37	GPR160	PBK
LRRC7	MTMR8	COL16A1	ZBTB41	FBXO28	GAR1	CSRP2	C5orf24	COMMD10	SUCLG2	AGPAT5
CCT8P1	TBX22	DLGAP3	UHMK1	CBX3	MBNL1	UBE3A	PPP2R5A	TRHDE	SRPK2	RYK
FMO1	NOX1	EDN2	TMED7	APPL1	ANKIB1	PGRMC2	NDUFA5	KRR1	RAD51AP1	ZNF704
HSPE1P6	EIF4BP7	H2AC20	PAWR	CCSAP	ZMPSTE24	OTUD6B	PHTF2	VASH2	BNIP3	ATAD1
RPS15AP12	HAX1P1	MPZ	CDC73	EIF2AK2	FAM91A1	DYRK2	PAPOLA	SMOC1	FANCM	UBP1
SRP9	MTMR7	PTPRVP	RAB21	KLHL24	ZNF148	IDE	FZD3	SMC4	AMD1	CRYZ
LDHAP3	TNFRSF10A-AS1	C2orf50	UCHL5	PPIP5K2	ZHX1	MIER3	ENAH	PAN3	CEP63	RMDN1
NRXN1	CIBAR1	IL36RN	MMP16	RRP15	UBN2	AGTPBP1	RC3H1	RAB4A	MRPL42	LEPROTL1
PRELID1P6	NACA4P	CCDC13	DEK	ECT2	MTDH	PRPF39	DCUN1D1	ARF4	SLAIN1	ZNF730
FHL2	RMRP	SETD7	TBL1XR1	HECA	CNOT7	ZNF780A	KIF5B	PTPN11	PBRM1	PIK3CB
SNRPGP9	FRMPD1	GMPR	BROX	BBX	LIN7C	EIF5A2	RAB3IP	G3BP2	PRKAA1	FGD5-AS1
DARS1-AS1	MIR4477B	RASA4DP	NEK7	ARPP19	LDHA	YWHAQ	RYBP	TMTC3	DLD	CAND1
EFHB	KLF9	CLDN23	ZBTB10	BRWD1	UBE2D3	TRNT1	YES1	CHML	ZNF800	EIF4G2
ERC2	FSD1L	CHCHD2P9	PPP1CB	PPP1CC	SMG1	EPM2AIP1	HOOK1	TMEM106B	GNAQ	FGD6
TF	C1QL3	LMX1B	BNIP3L	FEM1C	TOMM20	MAP3K1	KRAS	ARL8B	ZDBF2	SRSF1
ZBBX	ARL5B	ENTPD8	CGGBP1	RPRD1A	AEBP2	PRKAR2B	TAX1BP1	ASPM	FAM126A	EPS15
PEX5L	BMI1	IFIT2	HGF	CCDC91	HNRNPR	TSPAN8	PLEKHA8	DENR	SACM1L	OXSR1
CCDC39	RASSF4	CREB3L1	PPP3CA	SLC16A7	SLC2A13	POC1B	ATP6V1A	DR1	RHOBTB1	SNX6
B3GNT5	IPMK	MYO7A	ZDHHC2	NRAS	PUS7L	FST	SLC19A2	HNRNPH3	TFDP2	MTMR2
ABCA11P	EGR2	IGFBP6	LRRC58	MATR3	CASD1	CDK6	BBS10	FAM120A	PHF3	ELK4
SRD5A3-AS1	AIFM2	MIPEPP3	RALGPS2	AGO3	EFNB2	STRN3	PSIP1	SEMA3D	C2CD5	COMMD2
EPHA5	SRP9P1	NKX2-8	TMED5	NR1D2	SESTD1	CDC42SE2	CACNA2D1	LPGAT1	BCAP29	SMARCA5
UGT2B15	C11orf65	IGFALS	PTP4A1	PPP1R12A	TBC1D5	DENND6A	RRM2B	ZNF107	TC2N	TMEM126B
GPRIN3	SLC6A12	HIC1	TOP2B	TMEM263	PDE12	ACBD3	BMI1	TBC1D15	CBLL1	TRMT13
GRID2	ETFRF1	VMO1	LYPLA1	ZMAT3	TNKS	TMEM65	ACAP2	XPR1	PLOD2	PDS5A
DNAJB14	TSPAN11	GALR2	POU2F1	PARPBP	UBA3	LIN7A	GXYLT1	C21orf91	ZNF92	DIMT1
FAM241A	ALG10	ADAM33	CLASP2	ZNF678	IMPA1	ZNF680	NAA50	TMOD3	PPM1L	NCEH1
PCDH18	CCDC184	ADAT3	NUCKS1	BCLAF1	ATP11B	MFN1	LPP	RMI1	TES	ITGB8
CBR4	PRANCR	SYDE1	SLC25A36	RCOR3	ABHD10	FUBP1	EXOC5	FGFR1OP2	FOXJ3	SSX2IP
LRP2BP	TRHDE	IGLV1-51	PHIP	ALG10	G3BP1	PRKACB	ALCAM	IPO8	RAD21	BCAS2
FST	RPL34P27	LINC00634	LARP4	DDAH1	ABCB10	RCHY1	YWHAZ	XPO1	STAU2	STAG1
RPL26P19	COX17P1	IL17REL	DBF4	FMO1	SCRN1	ARIH1	KCTD3	RAB2A	SOAT1	TRMT10C
CMYA5	BCL2L2-PABPN1		ARPC5	ARHGAP11A	FAM8A1	LSM5	CMTM6	PGGT1B	PCM1	ZNF695
RASGRF2	GMFB		YOD1	NFAT5	ZNF518A	VPS13A	RNF141	FOXP1	KPNA4	UBE2K
POLR3G	DUOX1		TSNAX	CD2AP	ANKRD12	CHMP2B	ZDHHC17	UBE2W	KDM5B	PDCL
TMED7	EID1		PANK3	SOCS4	CPNE3	SPTSSA	DCUN1D4	ELMOD2	PEX2	PICALM
KRT8P33	IQCH		CPSF6	REST	REEP3	HLTF	ATAD2	TM9SF3	RABEP1	ARL15
RAPGEF6	TM6SF1		SRP9	OSBPL8	CEBPZOS	DTWD2	NDUFB5	SDCBP	KIF2A	SIRT1
CREBRF	RNU7-111P		DHX36	SKIL	CNST	PIGK	MDM4	NLGN1	APC	FAM135A
CPNE5	SMG1P1		NAP1L1	MYBL1	LMBR1	DNM1L	LBR	LYSMD3	HELLS	EHBP1
IMPG1	GAS8-AS1		PPP4R2	ZNF654	RSBN1L	KIAA1586	ETNK1	AGFG1	PRKCI	KBTBD8
FUT9	RPS27AP1		TWF1	DPY19L4	GOLT1B	USP14	ATP13A3	EEA1	PIK3CA	CCNE2
EEF1A1P6	ASXL3		TNPO1	CLDND1	CTDSPL2	GOLGA4	VAMP4	AVL9	LSM14A	UHRF1BP1L
HOXA9	IER3IP1		PTEN	GTPBP8	MKLN1	TBK1	TPD52	DESI2	ZNF281	DPY19L1
CASD1	FTLP3		WASL	RB1CC1	CCDC14	ACVR2B	AP3S1	CUL5	TMEM168	ERGIC2
TPI1P2	RPL12P4		PCNP	SEC62	TDRP	CEP290	MYO6	ATG12	PTGES3	ZDHHC20
EEF1B2P6	RPL12P41		THAP5	CEP97	NSUN3	C1GALT1	UBE2V2	PHACTR2	SCYL2	RBBP8
FAM131B	SNORD88A		TMPO	SRSF11	MME	TOPBP1	PPP1R2	POLR2M	SDE2	TMEM17
AP1S2	RPL13AP7		IPMK	CDK14	SMCHD1	AP5M1	ARID4B	TRIM33	PHC3	
	SH3BGR		XRN1	DENND1B	NAA15	UBQLN1				

Table S1. LIST of SETD7-regulated genes

SUPPLEMENTARY MATERIALS AND METHODS

List of ChIP-qPCR primers:

KLK3-ARE	Forward, 5'-GCCTGGATCTGAGAGAGATATCATC-3'
	Reverse, 5'-ACACCTTTTTTTTTCTGGATTGTTG-3'
NKX3.1-ARE	Forward, 5'-CTGGCAAAGAGCATCTAGGG-3'
	Reverse, 5'-GGCACTTCCTGAGCAAACTT-3'
FKBP5-ARE	Forward, 5'-CTCTCCAACCTGCACTCCAT-3';
	Reverse, 5'-TAAAAGCACACAGGCGTGAA-3'
ZBTB16-ARE	Forward, 5'-ACACCATGGCCTGTTGTAAA-3'
	Reverse, 5'-AAAACAGCAGACCCAAA-3'
RAB11B-FXBS	Forward, 5'-ACTTACAGCAATGATGGGGAC-3'
	Reverse, 5'- CCTGACCCATTGATCTGTTTGT-3'
CDK1-FXBS	Forward, 5'-TGCCTATCAGTAGTGCCCAA-3'
	Reverse, 5'-GTTCAGAAGAGCAAACAAGGAA-3'
SPRY4-FXBS	Forward, 5'-GGCATCTGGCCTGGCATATAA-3'
	Reverse, 5'-AACACAATGCATGGCACACAG-3'
RET-FXBS	Forward, 5'-CCCAAGGCAGAGGGCATAAG-3'
	Reverse, 5'-CTGCTCGTCCTCTGAAAACCT-3'
RUFY1-FXBS	Forward, 5'-ACCAGCTTACTGGGTTTCAGAG-3'
	Reverse, 5'-CCCATTATCTTGTCGCATTGCC-3'
PDK1-FXBS	Forward, 5'-GGTCAGCAAAGGCAAATGGC-3'
	Reverse, 5'-CAAGGAAGCAAACAGCTGCC-3'
GRID2-FXBS	Forward, 5'-CTTGCAGCCTTTTCTGCGTT-3'
	Reverse, 5'-AGAACACCAAGCCATGCGTA-3'
ALG10-FXBS	Forward, 5'-GTTTTGACACTTTGTGCGCC-3'
	Reverse, 5'-GGATCCGGAAAGATCGGGTC-3'
ACVR1C-FXBS	Forward, 5'-GGAGCCTCCGGGACTAGATA-3'
	Reverse, 5'-CAATCGCCGCGTAGTTGAAG-3'
NDC80-FX2BS	Forward, 5'-GCCATGAGTCACAGAAGGTTG-3'
	Reverse, 5'-TCAGTGATAACCATACCAAACTGG-3'
TP63-FX2BS	Forward, 5'-ACTCATCTGTTTACCTTTTGCTGT-3'
	Reverse, 5'-TGTGGTTCTGAGGCTGAGTG-3'
WNT7A-FX2BS	Forward, 5'-GCGTCAGTGAATGGTTGCTG-3'
	Reverse, 5'-AAACTGGTTCCTGCCATCAG-3'
CDK1-FX2BS	Forward, 5'-AAACAGCCTTCCAGGGAGTG-3'
	Reverse, 5'-ATCCAAGTCAAAGGTAGCTGGA-3'

List of shRNAs:

shSETD7-1	Target sequence 5'-AATCCGTCATCGTCCAGGT-3'
shSETD7-2	Target sequence 5'-AAATTTCCCATAAAGTGCG-3'

List of antibodies used for immunoblotting

Cells were boiled with 2%SDS, and proteins were detected with primary antibodies, including anti-V5 (Abcam, ab9116), anti-MLL1 (Abcam, ab243867), anti-FOXA1 (Abcam, ab23738), anti-SETD7 (CST, 2813S), anti-CoREST (Abcam, ab183711), anti-GAPDH (Abcam, ab8245), anti-H3K4me1(Abcam, 8895), anti-H3K4me2 (Millipore, 07-030), anti-H3K27ac (Abcam, ab4729), and anti-IgG (Millipore, 12-370). The gels shown are representative of at least three independent experiments.

ChIP-seq Analysis:

For ChIP preparation, cells were fixed with 1% formaldehyde and lysed by the ChIP lysis buffer (1% SDS, 5mM EDTA, 50mM Tris–HCl pH 8.1). Chromatin was sheared to ~500-800bp fragments (for ChIP-qPCR) or ~300bp fragments (for ChIP-seq) using the Bioruptor Sonicator (Diagenode). Immunoprecipitation was performed using ChIP grade antibodies. The precipitated protein-DNA complexes were then reverse-crosslinked at 65^{o}C, followed by DNA purification. The extracted DNA was subjected to ChIP-qPCR (primers are listed above) using the SYBR green method or ChIP-seq analysis. ChIP-seq libraries were constructed using the SMARTer ThruPLEX DNA-Seq Prep Kit (Takara Bio USA). Next-generation sequencing (51nt, single-end) was performed using Illumina HiSeq2500**.** ChIP-sequencing reads were mapped to the hg19 human genome using bwa (version 0.7.17-r1188) with aln and sampe sub-commands. Samtools (version 1.9) was used to convert SAM files to BAM format. The significance of enriched ChIP peaks was evaluated using MACS2 (version 2.1.4) (7). The Intervene (version 0.6.5) was used to analyze peak intervals, determine overlapped regions, and generate Venn diagrams. The signals associated with genomic regions were visualized using compueMatrix and plotHeatmap tools from deepTools (version 3.3.0). computeMatrix with reference-point mode was used to calculate scores for each genomic region, and plotHeatmap was used to create a heatmap for scores associated with genomic regions. Motif enrichment analysis was performed by using SeqPos with the default setting. Binding and Expression

Target Analysis (BETA) was performed by BETA software package (version 1.0.7) with default parameters to integrate ChIP-seq with differential gene expression data to predict direct targets. Antibodies used for ChIP were anti-SETD7 antibody (Cell signaling, 2813s), anti-FOXA1 (Abcam, ab23738), and anti-V5 (Thermo Fisher Scientific).

RNA-seq Analysis:

RNA was extracted from cell lines with TRIzol reagent (Invitrogen) and RNA from tumor tissue samples was extracted using TissueLyser LT (Qiagen) and RNeasy Kit (Qiagen). Quantitative real-time PCR (qRT-PCR) was performed using Fast 1-step Mix (Thermo Fisher Scientific) on a QuantStudio 3 PCR machine. All qRT-PCR results were normalized to GAPDH and quantitated using ΔΔCt method. Taqman primers and probes for *SETD7*, *GRID2*, *ALG10*, *ACVR1C*, and *GAPDH* were predesigned and obtained from Thermo Fisher Scientific. For RNA-seq, the library preparation was performed using the TruSeq Strand Total RNA LT (Illumina). Next-generation sequencing (51nt, single-end) was performed using Illumina HiSeq2500. Transcriptome-sequencing reads were aligned to the human reference genome (hg19) using STAR (version 2.7.1a) and counted with featureCounts (version 2.0.1) from GRCh37 Ensembl reference. All gene counts were processed with the R package Edger (3.36.0) to evaluate differential expression using the Benjamini–Hochberg false discovery rate (FDR)-adjusted *P*-value. The expression values were centered and scaled across samples and then displayed using the ComplexHeatmap (version 2.10.0) R package. Volcano plot analysis was performed using SeqPos with the default setting in Galaxy/Cistrome. Gene Set Enrichment Analysis (GSEA) was conducted using the GSEA software (version 4.2.2) and the R package fgsea (version 1.20.0).

ADDITIONAL REFERENCES

1. C. Gerhauser *et al.*, Molecular Evolution of Early-Onset Prostate Cancer Identifies Molecular Risk Markers and Clinical Trajectories. *Cancer Cell* **34**, 996-1011 e1018 (2018).
2. A. Kamoun *et al.*, Comprehensive molecular classification of localized prostate adenocarcinoma reveals a tumour subtype predictive of non-aggressive disease. *Ann Oncol* **29**, 1814-1821 (2018).
3. C. Cai *et al.*, ERG induces androgen receptor-mediated regulation of SOX9 in prostate cancer. *J Clin Invest* **123**, 1109-1122 (2013).

4. S. Gao *et al.*, Chromatin binding of FOXA1 is promoted by LSD1-mediated demethylation in prostate cancer. *Nat Genet* **52**, 1011-1017 (2020).
5. W. Han *et al.*, Exploiting the tumor-suppressive activity of the androgen receptor by CDK4/6 inhibition in castration-resistant prostate cancer. *Mol Ther* **30**, 1628-1644 (2022).
6. M. D. Nyquist *et al.*, Combined TP53 and RB1 Loss Promotes Prostate Cancer Resistance to a Spectrum of Therapeutics and Confers Vulnerability to Replication Stress. *Cell Rep* **31**, 107669 (2020).
7. Y. Zhang *et al.*, Model-based analysis of ChIP-Seq (MACS). *Genome Biol* **9**, R137 (2008).